Published in final edited form as:

J Cell Physiol. 2018 August ; 233(8): 5503–5512. doi:10.1002/jcp.26418.

Mesenchymal stromal cells prevent bleomycin-induced lung and skin fibrosis in aged mice and restore wound healing

Gustavo A. Rubio[1], **Sharon J. Elliot**[1], **Tongyu C. Wikramanayake**[2], **Xiaomei Xia**[3], **Simone Pereira-Simon**[1], **Seth R. Thaller**[1], **George D. Glinos**[2], **Ivan Jozic**[2], **Penelope Hirt**[2], **Irena Pastar**[2], **Marjana Tomic-Canic**[2], **Marilyn K. Glassberg**[1,3]

[1]DeWitt Daughtry Family Department of Surgery, University of Miami Leonard M. Miller School of Medicine, Miami, Florida

[2]Wound Healing and Regenerative Medicine Research Program, Department of Dermatology and Cutaneous Surgery, University of Miami Leonard M. Miller School of Medicine, Miami, Florida

[3]Department of Medicine, University of Miami Leonard M. Miller School of Medicine, Miami, Florida

Abstract

Fibrosis can develop in nearly any tissue leading to a wide range of chronic fibrotic diseases. However, current treatment options are limited. In this study, we utilized an established aged mouse model of bleomycin-induced lung fibrosis (BLM) to test our hypothesis that fibrosis may develop simultaneously in multiple organs by evaluating skin fibrosis and wound healing. Fibrosis was induced in lung in aged (18–22-month-old) C57BL/6 male mice by intratracheal BLM administration. Allogeneic adipose-derived mesenchymal stromal cells (ASCs) or saline were injected intravenously 24 hr after BLM administration. Full thickness 8-mm punch wounds were performed 7 days later to study potential systemic anti-fibrotic and wound healing effects of intravenously delivered ASCs. Mice developed lung and skin fibrosis as well as delayed wound closure. Moreover, we observed similar changes in the expression of known pro-fibrotic factors in both lung and skin wound tissue, including miR-199 and protein expression of its corresponding target, caveolin-1, as well as phosphorylation of protein kinase B. Importantly, ASC-treated mice exhibited attenuation of BLM-induced lung and skin fibrosis and accelerated wound healing, suggesting that ASCs may prime injured tissues and prevent end-organ fibrosis.

Correspondence: Marilyn K. Glassberg, MD, Division of Department of Medicine, University of Miami Leonard M. Miller School of Medicine, 1600 NW 10th Ave RMSB 7056 (D-60), Miami, FL 33136. mglassbe@med.miami.edu, Marjana Tomic-Canic, PhD, Department of Dermatology and Cutaneous Surgery, University of Miami Leonard M. Miller School of Medicine, 1600 NW 10th Ave RMSB 2023A, Miami, FL 33136. mtcanic@med.miami.edu.

AUTHORS' CONTRIBUTIONS

SJE, IP, SRT, MTC, SRT, and MKG conceived and designed the study. GAR, TW, XX, SPS, GDG, IJ, and PH performed experiments and data acquisition. GAR, SJE, TW, IP, MTC, and MKG performed data analysis and interpretation. GAR, SJE, SRT, IP, MTC, and MKG participated in manuscript writing and critical revisions. All authors read and approved final manuscript. Dr. Glassberg serves as a consultant expert on advisory boards for Genentech, Boehringer Ingelheim, Patara Pharma, and Bellerophon Therapeutics.

All other authors have indicated no conflict of interest.

SUPPORTING INFORMATION

Additional Supporting Information may be found online in the supporting information tab for this article.

Keywords

fibrosis; MSC; wound healing

1 | INTRODUCTION

Aberrant wound healing resulting in fibrosis can occur in nearly all tissues and organ systems leading to a wide variety of chronic diseases that together account for nearly a third of worldwide disease-related mortality (Rockey, Bell, & Hill, 2015; Wynn, 2008; Zeisberg & Kalluri, 2013). Despite representing a major global health issue, few, if any, effective anti-fibrotic therapies are available to date. Thus, there is a great clinical need to better understand the mechanisms involved in fibrosis and to develop effective and safe therapies. This aberrant fibrogenic process is thought to involve common cellular and molecular pathways (Rockey et al., 2015; Zeisberg & Kalluri, 2013). Such pathways may be involved in fibrotic diseases in multiple organs and, therefore, represent an attractive target for novel anti-fibrotic therapies.

The fibrogenic cascade may be initiated by a variety of stimuli resulting in tissue injury such as infections, autoimmune reactions, radiation, or chemical injury (Wynn, 2008). Furthermore, aging plays an important role and is one of the prominent contributing factors. In response to injury, a complex inflammatory reaction ensues that under normal conditions is adaptive and results in normal wound healing (Rockey et al., 2015). In certain disease states and in aging, a phenotypic reprogramming may occur in cells leading to an imbalance between extracellular matrix (ECM) deposition and resorption, resulting in tissue fibrosis (Rockey et al., 2015; Usunier, Benderitter, Tamarat, & Chapel, 2014; Wynn, 2008; Zeisberg & Kalluri, 2013). A goal of anti-fibrotic therapies is, therefore, to restore an “acute repair phenotype” in fibrotic tissues to promote healing and tissue restoration.

Appropriate pre-clinical models are necessary to study potential systemic anti-fibrotic therapies that may target common pathways and have beneficial effects in multiple tissues. Among established animal models of fibrosis, bleomycin (BLM) has been used to induce lung and skin fibrosis (Ishikawa, Takeda, Okamoto, Matsuo, & Isobe, 2009; Marangoni, Varga, & Tourtellotte, 2016; Tashiro et al., 2015; Wu & Varga, 2008). BLM causes chelation of metal ions and oxygen free radical production leading to DNA breaks and tissue injury resulting in fibrosis (Moeller, Ask, Warburton, Gauldie, & Kolb, 2008). Rodent models of intratracheal BLM-induced lung fibrosis have been implemented to study idiopathic pulmonary fibrosis (IPF) (Moeller et al., 2008; Peng et al., 2013). Additionally, subdermal BLM injections have been used to induce skin fibrosis and mimic some of the manifestations of scleroderma (Ishikawa et al., 2009; Lee et al., 2014; Liang et al., 2015; Marangoni et al., 2016). Furthermore, BLM can be used to induce injury to multiple organs, as demonstrated with repeated high doses of subcutaneous BLM causing skin, lung, and gastrointestinal injury (Ishikawa et al., 2009). Therefore, BLM injury resulting in skin and lung fibrosis may provide a pre-clinical model to study potential systemic anti-fibrotic therapies that target multiple organs.

Among potential systemic anti-fibrotic therapies under investigation, mesenchymal stem/stromal cells (MSCs) have emerged as one of the most promising. MSCs have been shown to exert anti-inflammatory, anti-oxidant, and immunomodulatory effects, as well as an ability to modulate pro-fibrotic factors (Eming, Martin, & Tomic-Canic, 2014; Toonkel, Hare, Matthay, & Glassberg, 2013; Usunier et al., 2014). MSCs have been investigated in pre-clinical and clinical studies for diseases in various organs including the heart (Chen et al., 2016), lung (Glassberg et al., 2016), kidney (Wang et al., 2016), liver (Haldar, Henderson, Hirschfield, & Newsome, 2016), and skin (Ojeh, Pastar, Tomic-Canic, & Stojadinovic, 2015; Otero-Vinas & Falanga, 2016). Benefits of MSCs in various organs are thought to stem from their ability to adapt to the local environment and regulate its secretome (Usunier et al., 2014). Thus, one potential advantage of MSCs, in contrast to individual anti-fibrotic drugs, is their ability to act on several pathways simultaneously and orchestrate a phenotypic reprogramming. One such way that MSCs may exert anti-fibrotic effects and restore an “acute repair phenotype” is by modulating several pathways simultaneously via delivery of microRNAs (Baglio et al., 2015; Wang et al., 2016).

In this study, we utilized an established aged mouse model of BLM-induced, non-reversible, lung fibrosis (Tashiro et al., 2015) to test our hypothesis that fibrogenesis may develop simultaneously in multiple organs by evaluating skin fibrosis and its impact on wound healing. Furthermore, we utilized this model to evaluate the potential of systemic allogeneic MSC administration to restore an “acute repair phenotype,” attenuate fibrosis and promote simultaneous cutaneous wound healing and lung repair by modulating pro-fibrotic factors. We induced pulmonary fibrosis in aged (18–22-month-old) male C57BL/6 by intratracheal BLM followed by full thickness 8-mm punch biopsy wounds 7 days later, coinciding with the onset of pulmonary fibrosis (Izbicki, Segel, Christensen, Conner, & Breuer, 2002). Allogeneic adipose-derived mesenchymal stromal cells (ASCs) or saline were injected intravenously 24 hr after BLM administration. At 14 days post-wounding, lungs, and cutaneous wound tissue were collected for functional and molecular assessments. We demonstrate that mice subjected to BLM-induced lung fibrosis also exhibited skin fibrosis and delayed wound closure. Moreover, we demonstrated similar changes in lung and skin wound tissue in the expression of known pro-fibrotic factors, including miR-199, and corresponding protein expression of its target, caveolin-1 (CAV-1), as well as phosphorylation of protein kinase B (AKT), all of which have been implicated in molecular pathways of fibrosis (Castello-Cros et al., 2011; Lino et al., 2013; Mercer et al., 2016b). Lastly, ASC-treated mice exhibited attenuation of BLM-induced lung and skin fibrosis and accelerated wound healing, suggesting that ASCs may prime injured tissues and prevent the end-organ fibrosis.

2 | METHODS

2.1 | Aged murine model of BLM-induced lung injury and delayed wound healing

All experiments were performed in accordance with approved guidelines and regulations. All experiments and procedures were approved by the Institutional Animal Care and Use Committee at the Leonard M. Miller School of Medicine at the University of Miami (Miami, FL), a facility accredited by the American Association for the Accreditation of Laboratory

Animal Care (protocol 13–131). Male C57BL/6 mice were obtained from Jackson Laboratories (Bar Harbor, ME). Aged (18–22-month-old) male mice were used for all experiments (n = 6/group). ASCs were isolated from young (4-month-old) male C57BL/6 donors (Tashiro et al., 2015). Animals were housed under pathogen-free conditions with food and water ad libitum.

2.2 | BLM-induced lung injury

Pulmonary fibrosis was induced by intratracheal BLM administrated as previously reported (Tashiro et al., 2015). In brief, mice were anesthetized with ketamine (200 mg/kg) and xylazine (10 mg/kg) injected intraperitoneally, followed by direct intratracheal instillation of bleomycin sulfate (Sigma–Aldrich Corp; St. Louis, MO) dissolved in 50 μl sterile saline (2.0 U/kg of bodyweight). Control mice received 50 μl of intratracheal sterile saline. One day following BLM or saline admnistration, mice were treated with either ASC or saline intravenous injection as described below.

2.3 | Wounding

Mice were wounded on day 7 after BLM or saline administration. Mice were again anesthetized with ketamine and xylazine injected intraperitoneally. Hair on the dorsal skin was removed with a clipper, and the skin was cleaned with providone-iodine antiseptic solution. A circular full-thickness wound was induced along the dorsal midline with an 8-mm punch, and covered with transparent film dressing (Tegaderm™, 3M, St. Louis, MO) for 24 hr, then exposed to room air. Mice were monitored daily and were euthanized 14 days later (21 days after BLM/saline treatment) and their lungs and skin wound tissue were harvested for analyses. Wound tissue and skin on the dorsal midline away from the wound sites were collected and bisected along the dorsal midline. Half of the specimens were fixed in 10% phosphate-buffered formalin and the other half were snap frozen for RNA and protein analyses.

2.4 | ASC isolation from young male donors

Donor ASCs were isolated from the subcutaneous adipose pads of 4-month-old male C57BL/6 mice, as previously described (Tashiro et al., 2015). Briefly, subcutaneous adipose tissue was excised, washed in phosphate buffer solution (PBS) without Ca^{2+} and Mg^{2+} (PBS) containing 30% GIBCO® Pen/Strep (Life Technologies; Grand Island, NY) and digested in media containing 0.75% type II collagenase (Sigma–Aldrich). Adipocytes were separated from the stromal vascular fraction by centrifugation. Resultant pellet was resuspended and cultured in ADSC™ Growth Medium (Lonza Group Ltd; Basel, Switzerland) and expanded in plastic Thermo Scientific™ Nunc™ Cell Culture Treated Flasks with Filter Caps (Thermo Fisher Scientific, Inc., Waltham, MA). Cells were incubated for 24 hr, at which point non-adherent cells were removed. Once cells reached confluency, they were trypsinized, expanded for 2–3 passages and cryopreserved in Recovery™ Cell Culture Freezing Medium (Life Technologies).

Characterization of ASCs was performed as previously described (Tashiro et al., 2015). Briefly, ASCs were incubated with fluores-cence-labeled antibodies and analyzed by flow-assisted cell sorting (FACS) Canto™ II (BD Biosciences; San Jose, CA). For mesenchymal

differentiation potential, Mouse Mesenchymal Stem Cell Functional Identification Kit (R&D Systems Inc.; Minneapolis, MN) was used according to the manufacturer's instructions. Pluripotency was assessed via osteogenic and adipogenic differentiation (Aguilar et al., 2009).

2.5 | ASC injections

Young donor-derived ASCs (passage 2 or 3) were thawed in a 37 °C water bath and washed in PBS to remove the cell freezing solution prior to injection. ASCs were then passed through a 70 μm cell strainer to remove cell clumps. Cells were counted and resuspended in PBS immediately prior to injection. One day following BLM or saline administration, mice were administered 5×10^5 ASCs in 200 μl of PBS by tail vein injection over 1 min. Control mice received 200 μl of saline by tail-vein injection.

2.6 | Lung histological analysis and Ashcroft scoring

Right lungs were inflated with 10% neutral buffered formalin (NBF) under 25 cm H_2O constant pressure. Lungs were fixed in 10% NBF overnight and then transferred to PBS at 4°C. Samples were embedded in paraffin and 4 μm sections were taken for hematoxylin-eosin (H&E) and Masson's Trichrome staining. Pulmonary fibrosis was assessed by a pathologist blinded to the experimental groups using the numerical Ashcroft scale (Ashcroft, Simpson, & Timbrell, 1988) on Masson's Trichrome-stained slides at 20× magnification. Individual fields were assessed by systematically moving over a 32-square grid; each field was assessed for severity of fibrosis and assigned a score of 0 (normal lung) to 8 (total fibrosis of the field).

2.7 | Histomorphometric analyses of skin fibrosis and acute wound healing

Formalin-fixed samples from skin adjacent to wounds were embedded in paraffin and 6-μm sections were stained with Picrosirius Red reagents following manufacturer's protocols (Electron Microscopy Sciences, Hatfield, PA). Representative images were captured on a Nikon Eclipse E400 microscope with polarized light (Nikon Inc., Melville, NY). Formalin-fixed wound samples were also embedded in paraffin and 6-μm sections were taken for H&E and Masson Trichrome staining. Representative images were captured on a Zeiss Observer D1 microscope (Carl Zeiss Microimaging Inc., Thornwood, NY). Total wound size (distance between normal connective tissues flanking the wound scar) and wound gap (distance between the migrating epithelial tongues) were measured and analyzed in each treatment group.

2.8 | Western blotting

Lung and skin wound tissue were homogenized and lysates were collected for Western blot analyses, as previously described (Tashiro et al., 2015). Protein lysates were loaded onto 10% polyacrylamide gels for analysis of AKT (10 μg), pAKT (25 μg), and CAV-1 (10 μg) protein expression. Primary antibodies and concentrations used were as follows: goat polyclonal anti-AKT1/2 N19 (1:1,000) (Santa Cruz Biotechnology, Dallas, TX), rabbit polyclonal anti-pAKT S473 (1:1,000), and rabbit polyclonal anti-caveolin-1 3238S (1:2,000) (Cell Signaling Technology, Danvers, MA). Immunoreactive bands were determined by

exposing nitrocellulose blots to a chemiluminescence solution (Denville Scientific Inc.; Metuchen, NJ) followed by exposure to Amersham Hyperfilm ECL (GE Healthcare Limited; Buckinghamshire, UK). ImageJ version 1.48v (National Institutes of Health; Bethesda, MD) was used to determine relative density of bands. β-actin expression was determined using mouse monoclonal anti-β-actin (1:10,000) (Sigma–Aldrich). All values were corrected for corresponding β-actin band.

2.9 | Real-time polymerase chain reaction (RT-PCR)

RT-PCR was performed to determine the expression levels of miR-199–3p, as well as mRNA expression of αv-integrin and TNFα. Total RNA was extracted from lung and skin wound tissue homogenates. Amplification and measurement of target RNA was performed on the Step 1 real time PCR system, as previously described (Karl, Berho, Pignac-Kobinger, Striker, & Elliot, 2006). TaqMan probes and primers for amplification of the specific transcripts were designed using the Primer Express 1.5 from Applied Biosystems (Foster City, CA). TaqMan ribosomal RNA control reagents (Life Technologies, Carlsbad, CA) designed to detect *18S* ribosomal RNA, were used as an endogenous control. For miR-199–3p analysis, cDNA was generated using qScript™ microDNA cDNA Synthesis Kit (Quanta Biosciences, Beverly, MA) according to manufacturer's instructions. Amplification of miR199–3p was performed using specific primers (IDT Biologika, Rockville, MD) using Real-Time SYBR Green qRT-PCR Amplification kit (Quanta Biosciences). *U6* expression was used as a control for miR199 analysis, and relative expression was calculated using the comparative CT method (Schmittgen & Livak, 2008).

2.10 | Statistical analysis

All values are expressed as mean ± standard error of the mean (SEM). Overall significance of differences within experimental groups was determined by analysis of variance (ANOVA) in combination with Tukey's multiple comparison test. Significance of differences between groups was determined using Student's *t*-tests, with Welch's correction as appropriate; p values less than 0.05 were considered statistically significant.

3 | RESULTS

3.1 | Single-dose intratracheal BLM-induced pulmonary fibrosis results in skin fibrosis and delayed wound healing in aged C57BL/6 mice

It has previously been shown that BLM-induced pulmonary fibrosis is less severe and can spontaneously resolve in young mice, an effect not observed in aged mice (Redente et al., 2011; Sueblinvong et al., 2012). Therefore, in this study we used the previously established aged mouse model of BLM-induced pulmonary fibrosis (Tashiro et al., 2015) to assess whether these mice also develop skin fibrosis leading to wound healing impairment. Significant fibrosis was observed by 21-day sacrifice in lung histological sections of BLM-treated mice compared to saline-treated controls (Figure 1a). Ashcroft scores, a semi-quantitative measure of lung fibrosis on histological sections (Ashcroft et al., 1988), were significantly increased in BLM-treated compared to saline-treated group (Figure 1b). Standard picrosirius red staining was used to analyze the systemic effects of BLM on collagen network alterations on intact dorsal (unwounded) skin. In saline-treated mice,

collagen fibers were long and well-aligned in a normal orientation parallel to the epidermis (Figure 1f). In BLM-treated mice, however, collagen fibers were shortened and misaligned, including areas where they were perpendicular to the epidermis (Figure 1f), which is consistent with skin fibrosis (Vorstenbosch et al., 2013). Moreover, histomorphometric analyses of wound healing including total wound size (distance between normal connective tissues flanking the wound scar) and wound gap (distance between the migrating epithelial tongues) were measured using H&E stained sections 14 days post-wounding. BLM treatment resulted in impaired wound healing, compared to the saline-treated control mice that exhibited normal wound healing (Figure 1c). Total wound size was approximately threefold larger in BLM-treated mice compared to saline-treated mice (Figure 1d; $p > 0.01$). Similarly, there was a sixfold increase in the size of wound gap in BLM-treated mice relative to saline-treated mice (Figure 1e; $p < 0.01$). These results demonstrate a significant delay in wound healing in mice with BLM-induced lung injury.

3.2 | Single-dose intravenous ASC treatment prevents lung and skin fibrosis and accelerates wound healing in BLM-treated aged mice

We have previously shown that allogeneic young male donor-derived ASCs can prevent the development of pulmonary fibrosis following intratracheal BLM instillation in aged mice (Tashiro et al., 2015). Given that ASCs appear to exert therapeutic effects in multiple organs and may modulate common fibrogenic pathways, we hypothesized that systemic ASC treatment may also prevent skin fibrosis and enhance wound healing in mice with BLM-induced pulmonary fibrosis by restoring an “acute repair phenotype” in injured tissues. Similar to our previous study, intravenous ASC treatment prevented the development of BLM-induced lung fibrosis that was observed in saline-injected mice (Figures 1a and 1b). ASC treatment also prevented the pathological effects of BLM on skin collagen fibers, as demonstrated by well-aligned collagen fibers parallel to the epidermis similar to the collagen network observed in saline-treated control mice (Figure 1f). Furthermore, ASC treatment prevented an impairment in wound healing in mice subjected to BLM-injury (Figure 1c), as evidenced by a significant reduction in the total wound size by 58.8% compared to wounds of saline-injected mice (Figure 1d; $p < 0.01$). Similarly, ASC-treated mice had a wound gap size 69.5% smaller compared to saline-treated mice (Figure 1e; $p < 0.05$).

3.3 | Profibrotic miR-199–3p expression is increased in lung and skin wounds of BLM-treated mice, an effect prevented by systemic ASC treatment

MicroRNAs (miRs) are major regulators of gene expression that have been shown to target key genes in pro-fibrotic pathways common to several organs (Bowen, Jenkins, & Fraser, 2013). Thus, miR regulation represents an attractive approach to modulate pro-fibrotic pathways. Moreover, delivery of beneficial miRs has been proposed as a mechanism by which MSCs exert their anti-fibrotic effects (Wang et al., 2016). Among several pro-fibrotic miRs, miR-199–3p has been reported to be upregulated in lung, kidney, and liver fibrosis (Lino et al., 2013). MiR-199–3p has also been implicated in cutaneous wound healing response (Chan, Roy, Huang, Khanna, & Sen, 2012). Therefore, we examined miR-199–3p expression in lung and cutaneous wound tissue in our study, and found an upregulation of miR-199–3p in both tissues (Figure 2) in BLM-treated mice compared to saline controls ($p < 0.01$). Mice treated with systemic ASCs following BLM-injury had lower expression of

miR-199–3p in both skin wound tissue (Figure 2a) and lungs (Figure 2b) compared to saline-treated mice.

3.4 | CAV-1 protein expression downregulation in lung and skin wounds of BLM-treated mice was prevented by systemic ASC treatment

Given the observed upregulation of miR-199–3p expression following BLM injury and its prevention by ASC treatment, we next sought to examine if protein expression of a confirmed target of miR-199–3p, CAV-1(Lino et al., 2013), was also modulated. CAV-1 is an important structural molecule often involved in sequestering growth factor receptors and blocking their signaling from the plasma membrane. Moreover, CAV-1 is downregulated in fibrotic skin (Castello-Cros et al., 2011; Lino et al., 2013) and lung diseases (Castello-Cros et al., 2011). Western blot analysis showed that ASC treatment resulted in a prevention of the CAV-1 downregulation that was observed in skin and lungs of BLM-treated mice (Figure 3).

3.5 | BLM-induced activation of AKT pathway in lung and skin wounds of aged mice was prevented by ASC treatment

Phosphorylation of AKT has been implicated in the signaling pathway of fibrogenesis (Mercer et al., 2016a). As expected, Western blot analysis showed that levels of phospho-AKT were increased in lung and skin wounds of BLM-treated mice compared to saline-treated controls (Figure 4). Importantly, this effect was prevented with systemic ASCs in both tissues in mice treated after intratracheal BLM administration (Figure 4).

3.6 | Molecular markers of inflammation and fibrosis are upregulated in lung and skin of aged mice by BLM, an effect prevented by ASC treatment

Real-time polymerase chain reaction (RT-PCR) was used to detect expression of tumor necrosis factor alpha (TNFα) and α_V-integrin. Results showed that treatment with ASCs prevented the significant upregulation of these markers associated with tissue inflammation and fibrosis in BLM-treated mice. TNF-α was increased in lung and skin wounds of BLM-treated mice compared to saline-treated controls indicating increased inflammation (Table 1; $p < 0.05$). ASC treatment prevented BLM-induced upregulation of TNF-α expression in both lung and skin wound tissue (Table 1; $p < 0.05$). Expression of α_V-integrin mRNA, a transmembrane cell adhesion molecule that modulates tissue fibrosis (Conroy, Kitto, & Henderson, 2016), was also increased in lung and skin from BLM-treated mice compared to saline controls (Table 1; $p < 0.01$ and $p < 0.05$, respectively). Similarly, systemic ASC infusion resulted in prevention of α_V-integrin mRNA upregulation in both lung and skin (Table 1; $p < 0.05$).

4 | DISCUSSION

Tissue fibrosis can affect nearly every organ system and represents a major global health challenge (Rockey et al., 2015). To date, there are limited treatment options to attenuate tissue fibrosis and prevent end-organ failure. Conditions such as aging and certain disease states can impair the normal tissue response to injury. This abnormal wound response may result in excessive ECM deposition leading to tissue fibrosis and healing impairment

(Kapetanaki, Mora, & Rojas, 2013; Rockey et al., 2015). Common molecular pathways appear to be involved in this fibrogenic cascade that can affect multiple organs. Pre-clinical models of multi-tissue fibrosis are, therefore, important to study novel therapies that target these common fibrotic pathways. In the present study, fibrosis was induced in lung and skin of aged mice by intratracheal BLM administration followed by wounding to study potential systemic anti-fibrotic and wound healing effects of cell-based therapy. Results suggest that systemic administration of allogeneic ASCs can restore an “acute repair phenotype” by modulating pro-fibrotic factors to prevent lung and skin fibrosis and promote wound healing.

One of the novel aspects of this study is the use of an aged murine model of BLM-induced lung and skin fibrosis with impaired healing. Given the similarities of aberrant healing and fibrogenic pathways, such as in patients with IPF and chronic venous leg ulcers (Blumberg et al., 2012; Eming et al., 2014), we postulated that BLM-induced lung fibrosis would result in dysregulation of repair mechanisms leading to fibrosis in skin tissue and impaired wound healing. BLM is a chemotherapeutic agent that can cause oxygen free radical production and DNA breaks that can result in tissue fibrosis (Moeller et al., 2008). This drug has been widely used to induce lung fibrosis in pre-clinical animal models (Moeller et al., 2008; Peng et al., 2013). Previous studies have also reported induction of both lung and skin fibrosis by repetitive or continuous subdermal administration of BLM (Lee et al., 2014; Liang et al., 2015). These studies suggest that BLM can result in tissue injury and fibrosis at the local site of administration and has systemic effects that can promote fibrosis in other tissues. However, these studies have used young mice, which, in contrast to aged mice, spontaneously recover from BLM-induced fibrosis (Redente et al., 2011; Tashiro et al., 2015). Moreover, to our knowledge, this is the first report of a murine model of simultaneous lung and skin fibrosis, as well as impaired wound healing, after a single-dose of intratracheal BLM. This model, thus, may facilitate investigation of anti-fibrotic therapies that can be applicable to patients with fibrotic conditions.

Fibrosis is the end-result of a complex cascade of events that involves dysregulation in multiple pathways and inflammatory effector cells (Wynn, 2008). It is unlikely, therefore, that drugs that target single molecules or pathways will lead to effective anti-fibrotic therapies (Wynn, 2011). Given the complexity of fibrosis and intricacies of the end-organ tissues it is particularly challenging to develop a single drug therapy that can simultaneously reverse fibrosis in multiple organs. Also, combination therapies may be less effective given the potential of additive side effects. Cell-based therapies, such as ASCs, have been studied as anti-fibrotic therapy in several organs (Chen et al., 2016; Glassberg et al., 2016; Haldar et al., 2016; Otero-Vinas & Falanga, 2016; Wang et al., 2016). ASCs appear to act by paracrine effects to modulate multiple pathways and demonstrate an ability to adapt to the local tissue to restore homeostasis and promote tissue repair (Usunier et al., 2014). In the current study, aged mice were treated with intravenous allogeneic ASCs one day following intratracheal BLM injury. Results suggest that systemic treatment with ASCs prevented BLM-induced lung and dermal fibrosis, and enhanced wound healing in aged mice. This suggests that ASCs may have the ability to systemically target common molecular pathways involved in fibrosis in different organs. It is tempting to speculate that in addition to aiding in tissue repair, ASCs given on day 1 may prime the end-organ tissues for prompt acute repair resulting in protective effects in this aged mouse model.

One mechanism by which ASCs may systemically regulate common fibrotic pathways is via modulation of miR expression in target tissues (Baglio et al., 2015; Wang et al., 2016). MiRs are small non-coding RNAs involved in post-transcriptional regulation of nearly 60% of all protein-encoding genes (Friedman, Farh, Burge, & Bartel, 2009; Pastar et al., 2012). Dysregulation of miRs has been implicated in fibrotic conditions including chronic skin wounds (Pastar et al., 2012) and lung fibrosis (Pandit & Milosevic, 2015). Overlap in multiple miRs dysregulated in different fibrotic conditions suggests that therapies that modulate their expression may be effective in reversing common fibrotic pathways and promoting tissue repair. In our study, we observed that the pro-fibrotic miR-199 was upregulated in both lung and skin wound tissue in BLM-treated mice. Notably, systemic ASC therapy prevented this miR-199 upregulation in both tissues. MiR-199 has been previously shown to be a key effector of fibrosis in multiple tissues including lung, kidney, and liver, via modulation of TGF-β signaling pathway and downregulation of CAV-1 expression (Lino et al., 2013). CAV-1 is a structural protein found in the caveolae of the plasma membrane (Castello-Cros et al., 2011). It is a bone fide target of miR-199 (Lino et al., 2013) and has been shown to be a key regulator of fibrosis in lungs (Drab et al., 2001; Wang et al., 2006; Yamaguchi, Yasuoka, Stolz, & Feghali-Bostwick, 2011) and skin (Castello-Cros et al., 2011). Importantly, induction of miR-199 and suppression of CAV-1 expression have also been reported in lungs of IPF patients (Lino et al., 2013; Wang et al., 2006). In the current study, changes in CAV-1 expression paralleled those of miR-199 in both skin and lung, with a downregulation in response to BLM that was prevented by ASC treatment. These results are consistent with previous studies that have shown a downregulation of CAV-1 expression in response to BLM-induced lung fibrosis in mice (Lino et al., 2013; Wang et al., 2006). Thus, results suggest that ASCs may prevent BLM-induced lung and skin fibrosis and promote wound healing by modulating the expression of miRs and its corresponding targets, which are involved in the fibrogenic pathway.

Other signaling pathways and effectors that are dysregulated in fibrosis were also evaluated and paralleled the results above. Activation of the AKT signaling pathway has been shown to be involved in tissue fibrosis (Mercer et al., 2016b; Russo et al., 2011). In addition, we previously showed that ASC treatment can prevent its activation in BLM-induced fibrotic lungs in aged mice (Tashiro et al., 2015). In the current study, AKT activation was increased in both skin and lung in BLM-treated mice, but this effect was prevented by ASC treatment. PI3K/AKT signaling pathway has been proposed as a potential therapeutic target in fibrotic conditions such as IPF (Mercer et al., 2016b), and these data support the claim that ASCs may, in part, alter the course of pulmonary fibrosis by modulating this pathway. Other markers of inflammation and fibrosis, α_V-integrin and TNFα, were also upregulated in lung and skin wound in response to BLM, and this was prevented by ASC therapy. These results further support the concept that ASCs appear to modulate multiple pathways involved in aberrant wound healing and fibrosis.

In summary, in the current study, lung and skin fibrosis was induced by a single intratracheal administration of BLM in aged mice, which also resulted in irreversible fibrosis and impaired wound healing. This pre-clinical model of fibrosis in two tissues may, therefore, be used to evaluate mechanism of action and effectiveness of novel systemic anti-fibrotic therapies. Moreover, results of this study support the hypothesis that ASC administration

may promote a systemic acute repair phenotype to prevent fibrosis in multiple organs and enhance wound healing by modulating pro-fibrotic factors such as miR-199 and its downstream target, CAV 1. These results highlight the potential of ASCs as systemic anti-fibrotic treatment that may act on multiple pathways and have therapeutic effects in multiple organs.

Supplementary Material

Refer to Web version on PubMed Central for supplementary material.

ACKNOWLEDGMENTS

We are grateful to all members of our laboratories for helpful criticisms and overall support. This work was funded by NIH grants NR013881 and NR015649 (MT-C). The authors also thank the Lester and Sue Smith Foundation and the James S. Fauver Pulmonary Fibrosis Research Fund for their generous support in research funding.

REFERENCES

Aguilar S, Scotton CJ, McNulty K, Nye E, Stamp G, Laurent G, …Janes SM (2009). Bone marrow stem cells expressing keratinocyte growth factor via an inducible lentivirus protects against bleomycin-induced pulmonary fibrosis. PLoS ONE, 4, e8013. [PubMed: 19956603]

Ashcroft T, Simpson JM, & Timbrell V (1988). Simple method of estimating severity of pulmonary fibrosis on a numerical scale. Journal of Clinical Pathology, 41, 467–470. [PubMed: 3366935]

Baglio SR, Rooijers K, Koppers-Lalic D, Verweij FJ, Perez Lanzon M, Zini N, … Pegtel DM (2015). Human bone marrow- and adipose-mesenchymal stem cells secrete exosomes enriched in distinctive miRNA and tRNA species. Stem Cell Research & Therapy, 6, 127. [PubMed: 26129847]

Blumberg SN, Maggi J, Melamed J, Golinko M, Ross F, & Chen W (2012). A histopathologic basis for surgical debridement to promote healing of venous ulcers. Journal of the American College of Surgeons, 215, 751–757. [PubMed: 22981433]

Bowen T, Jenkins RH, & Fraser DJ (2013). MicroRNAs, transforming growth factor beta-1, and tissue fibrosis. The Journal of Pathology, 229, 274–285. [PubMed: 23042530]

Castello-Cros R, Whitaker-Menezes D, Molchansky A, Purkins G, Soslowsky LJ, Beason DP, … Lisanti MP (2011). Scleroderma-like properties of skin from caveolin-1-deficient mice: Implications for new treatment strategies in patients with fibrosis and systemic sclerosis. Cell Cycle, 10, 2140–2150. [PubMed: 21670602]

Chan YC, Roy S, Huang Y, Khanna S, & Sen CK (2012). The microRNA miR-199a-5p down-regulation switches on wound angio-genesis by derepressing the v-ets erythroblastosis virus E26 oncogene homolog 1-matrix metalloproteinase-1 pathway. The Journal of Biological Chemistry, 287, 41032–41043. [PubMed: 23060436]

Chen H, Xia R, Li Z, Zhang L, Xia C, Ai H, … Guo Y (2016). Mesenchymal stem cells combined with hepatocyte growth factor therapy for attenuating ischaemic myocardial fibrosis: Assessment using multimodal molecular imaging. Scientific Reports, 6, 33700. [PubMed: 27804974]

Conroy KP, Kitto LJ, & Henderson NC (2016). Alphav integrins: Key regulators of tissue fibrosis. Cell and Tissue Research, 365, 511–519. [PubMed: 27139180]

Drab M, Verkade P, Elger M, Kasper M, Lohn M, Lauterbach B, … Kurzchalia TV (2001). Loss of caveolae, vascular dysfunction, and pulmonary defects in caveolin-1 gene-disrupted mice. Science, 293, 2449–2452. [PubMed: 11498544]

Eming SA, Martin P, & Tomic-Canic M (2014). Wound repair and regeneration: Mechanisms, signaling, and translation. Science Translational Medicine, 6, 265sr266.

Friedman RC, Farh KK, Burge CB, & Bartel DP (2009). Most mammalian mRNAs are conserved targets of microRNAs. Genome Research, 19, 92–105. [PubMed: 18955434]

Glassberg MK, Minkiewicz J, Toonkel RL, Simonet ES, Rubio GA, Difede D, … Hare JM (2016). Allogeneic human mesenchymal stem cells in patients with idiopathic pulmonary fibrosis via

intravenous delivery (AETHER): A phase I, safety, clinical trial. Chest, 151(2), 971–981. [PubMed: 27890713]

Haldar D, Henderson NC, Hirschfield G, & Newsome PN (2016). Mesenchymal stromal cells and liver fibrosis: A complicated relationship. FASEB Journal, 30, 3905–3928. [PubMed: 27601441]

Ishikawa H, Takeda K, Okamoto A, Matsuo S, & Isobe K (2009). Induction of autoimmunity in a bleomycin-induced murine model of experimental systemic sclerosis: An important role for CD4+ T cells. The Journal of Investigative Dermatology, 129, 1688–1695. [PubMed: 19158840]

Izbicki G, Segel MJ, Christensen TG, Conner MW, & Breuer R (2002). Time course of bleomycin-induced lung fibrosis. International Journal of Experimental Pathology, 83, 111–119. [PubMed: 12383190]

Kapetanaki MG, Mora AL, & Rojas M (2013). Influence of age on wound healing and fibrosis. The Journal of Pathology, 229, 310–322. [PubMed: 23124998]

Karl M, Berho M, Pignac-Kobinger J, Striker GE, & Elliot SJ (2006). Differential effects of continuous and intermittent 17beta-estradiol replacement and tamoxifen therapy on the prevention of glomerulo-sclerosis: Modulation of the mesangial cell phenotype in vivo. American Journal of Pathology, 169(2), 351–361. [PubMed: 16877338]

Lee R, Reese C, Bonner M, Tourkina E, Hajdu Z, Riemer EC, … Hoffman S (2014). Bleomycin delivery by osmotic minipump: Similarity to human scleroderma interstitial lung disease. American Journal of Physiology – Lung Cellular and Molecular Physiology, 306, L736–L748. [PubMed: 24583879]

Liang M, Lv J, Zou L, Yang W, Xiong Y, Chen X, … Zou H (2015). A modified murine model of systemic sclerosis: Bleomycin given by pump infusion induced skin and pulmonary inflammation and fibrosis. Laboratory Investigation, 95, 342–350. [PubMed: 25502178]

Lino Cardenas CL, Henaoui IS, Courcot E, Roderburg C, Cauffiez C, Aubert S, … Pottier N (2013). MiR-199a-5p Is upregulated during fibrogenic response to tissue injury and mediates TGFbeta-induced lung fibroblast activation by targeting caveolin-1. PLoS Genetics, 9, e1003291. [PubMed: 23459460]

Marangoni RG, Varga J, & Tourtellotte WG (2016). Animal models of scleroderma:Recent progress. Current Opinionin Rheumatology, 28,561–570.

Mercer PF, Woodcock HV, Eley JD, Plate M, Sulikowski MG, Durrenberger PF, … Chambers RC (2016a). Exploration of a potent PI3 kinase/mTOR inhibitor as a novel anti-fibrotic agent in IPF. Thorax, 71, 701–711. [PubMed: 27103349]

Mercer PF, Woodcock HV, Eley JD, Plate M, Sulikowski MG, Durrenberger PF, … Chambers RC (2016b). Exploration of a potent PI3 kinase/mTOR inhibitor as a novel anti-fibrotic agent in IPF. Thorax, 71, 701–711. [PubMed: 27103349]

Moeller A, Ask K, Warburton D, Gauldie J, & Kolb M (2008). The bleomycin animal model: A useful tool to investigate treatment options for idiopathic pulmonary fibrosis? International Journal of Biochemistry & Cell Biology, 40, 362–382. [PubMed: 17936056]

Ojeh N, Pastar I, Tomic-Canic M, & Stojadinovic O (2015). Stem cells in skin regeneration, wound healing, and their clinical applications. International Journal of Molecular Sciences, 16, 25476–25501. [PubMed: 26512657]

Otero-Vinas M, & Falanga V (2016). Mesenchymal stem cells in chronic wounds: The spectrum from basic to advanced therapy. Advances in Wound Care (New Rochelle), 5, 149–163.

Pandit KV, & Milosevic J (2015). MicroRNA regulatory networks in idiopathic pulmonary fibrosis. Biochemistry and Cell Biology, 93, 129–137. [PubMed: 25557625]

Pastar I, Khan AA, Stojadinovic O, Lebrun EA, Medina MC, Brem H, … Tomic-Canic M (2012). Induction of specific microRNAs inhibits cutaneous wound healing. The Journal of Biological Chemistry, 287, 29324–29335. [PubMed: 22773832]

Peng R, Sridhar S, Tyagi G, Phillips JE, Garrido R, Harris P, … Stevenson CS (2013). Bleomycin induces molecular changes directly relevant to idiopathic pulmonary fibrosis: A model for “active” disease. PLOS ONE, 8, e59348. [PubMed: 23565148]

Redente EF, Jacobsen KM, Solomon JJ, Lara AR, Faubel S, Keith RC, … Riches DW (2011). Age and sex dimorphisms contribute to the severity of bleomycin-induced lung injury and fibrosis.

American Journal of Physiology – Lung Cellular and Molecular Physiology, 301, L510–L518. [PubMed: 21743030]

Rockey DC, Bell PD, & Hill JA (2015). Fibrosis—A common pathway to organ injury and failure. New England Journal of Medicine, 372, 1138–1149. [PubMed: 25785971]

Russo RC, Garcia CC,Barcelos LS,Rachid MA, Guabiraba R, Roffe E, … Teixeira MM (2011). Phosphoinositide 3-kinase gamma plays a critical role in bleomycin-induced pulmonary inflammation and fibrosis in mice. Journal of Leukocyte Biology, 89, 269–282. [PubMed: 21048214]

Schmittgen TD, & Livak KJ (2008). Analyzing real-time PCR data by the comparative C(T) method. Nature Protocols, 3, 1101–1108. [PubMed: 18546601]

Sueblinvong V, Neujahr DC, Mills ST, Roser-Page S, Ritzenthaler JD, Guidot D, … Roman J (2012). Predisposition for disrepair in the aged lung. American Journal of the Medical Sciences, 344, 41–51. [PubMed: 22173045]

Tashiro J, Elliot SJ, Gerth DJ, Xia X, Pereira-Simon S, Choi R, … Glassberg MK (2015). Therapeutic benefits of young, but not old, adipose-derived mesenchymal stem cells in a chronic mouse model of bleomycin-induced pulmonary fibrosis. Translational Research, 166, 554–567. [PubMed: 26432923]

Toonkel RL, Hare JM, Matthay MA, & Glassberg MK (2013). Mesenchymal stem cells and idiopathic pulmonary fibrosis. Potential for clinical testing. American Journal of Respiratory and Critical Care Medicine, 188, 133–140. [PubMed: 23306542]

Usunier B, Benderitter M, Tamarat R, & Chapel A (2014). Management of fibrosis: The mesenchymal stromal cells breakthrough. Stem Cells International, 2014, 340257. [PubMed: 25132856]

Vorstenbosch J, Al-Ajmi H, Winocour S, Trzeciak A, Lessard L, & Philip A (2013). CD109 overexpression ameliorates skin fibrosis in a mouse model of bleomycin-induced scleroderma. Arthritis and Rheumatism, 65, 1378–1383. [PubMed: 23436317]

Wang B, Yao K, Huuskes BM, Shen HH, Zhuang J, Godson C, … Ricardo SD (2016). Mesenchymal stem cells deliver exogenous microRNA-let7c via exosomes to attenuate renal fibrosis. Molecular Therapy, 24, 1290–1301. [PubMed: 27203438]

Wang XM, Zhang Y, Kim HP, Zhou Z, Feghali-Bostwick CA, Liu F, … Choi AM (2006). Caveolin-1: A critical regulator of lung fibrosis in idiopathic pulmonary fibrosis. The Journal of Experimental Medicine, 203, 2895–2906. [PubMed: 17178917]

Wu M, & Varga J (2008). In perspective: Murine models of scleroderma. Current Rheumatology Reports, 10, 173–182. [PubMed: 18638424]

Wynn TA (2008). Cellular and molecular mechanisms of fibrosis. The Journal of Pathology, 214, 199–210. [PubMed: 18161745]

Wynn TA (2011). Integrating mechanisms of pulmonary fibrosis. The Journal of Experimental Medicine, 208, 1339–1350. [PubMed: 21727191]

Yamaguchi Y, Yasuoka H, Stolz DB, & Feghali-Bostwick CA (2011). Decreased caveolin-1 levels contribute to fibrosis and deposition of extracellular IGFBP-5. Journal of Cellular and Molecular Medicine, 15, 957–969. [PubMed: 20345844]

Zeisberg M, & Kalluri R (2013). Cellular mechanisms of tissue fibrosis. 1. Common and organ-specific mechanisms associated with tissue fibrosis. American Journal of Physiology Cell Physiology, 304, C216–C225. [PubMed: 23255577]

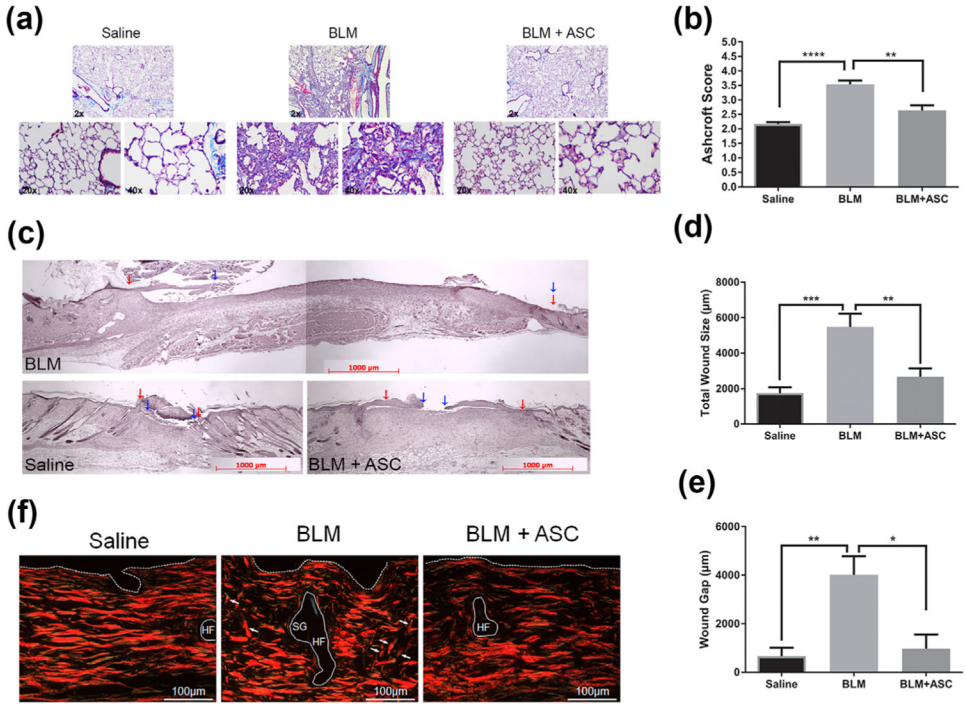

FIGURE 1.

Intratracheal bleomycin (BLM) results in lung and skin fibrosis, as well as delayed wound healing in aged mice, an effect prevented by systemic adipose-derived mesenchymal stromal cells (ASC) treatment. (a) Histological sections of lung tissue were stained with Masson's-Trichrome as described in section 2. Representative photomicrographs at 2× (upper), 20× (left), and 40× (right) magnification of lung sections from saline-treated control mice, BLM-treated mice, and BLM + ASCs. (b) Degree of pulmonary fibrosis on histological sections was measured by semi-quantitative Ashcroft score. BLM instillation resulted in increased Ashcroft score compared to saline controls. Treatment with ASCs following BLM administration resulted in decreased Ashcroft score. (c) Representative H&E staining of cutaneous wounds 14 days after induction. Red arrows indicate margin, and blue arrows indicate the epithelialized edges of the migrating tongues. Significantly increased total wound size (d) and wound gap (e) were observed in BLM-treated mice compared with saline-treated controls, suggestive of delayed healing. This delayed healing was prevented with ASC treatment (d,e). (f) Representative picrosirius red staining of intact skin 21 days after BLM treatment. BLM treatment resulted in altered collagen fiber morphology compared to saline-treated controls, and this effect was prevented in ASC-treated mice. White arrows indicate misaligned fibers. Dotted line denote basement membrane. HF: hair follicle; SG: sebaceous gland. Data are graphed as mean ± standard error of the mean ($n = 6$/group). *$p < 0.05$; **$p < 0.01$; ***$p < 0.001$; ****$p < 0.0001$. BLM, bleomycin

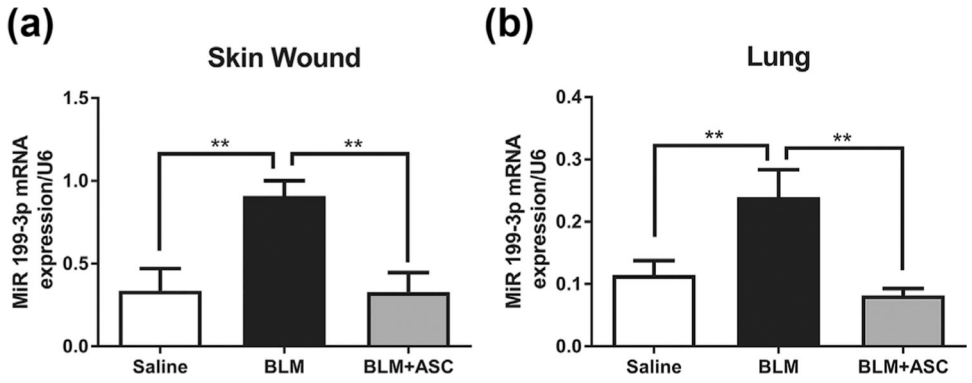

FIGURE 2.

Profibrotic miR-199–3p expression is increased in lung and skin wounds of bleomycin-treated mice, an effect prevented by systemic ASC treatment. Expression of miR-199–3p in skin wound (a) and lungs (b) of aged C57BL/6 mice is increased in response to BLM treatment compared to saline controls. Treatment with allogeneic ASCs 1 day post-BLM infusion resulted in lower expression of miR-199–3p, similar to that of saline-only controls. miR-199–3p expression was measured by reverse transcriptase polymerase chain reaction as described in Materials and Methods. *U6* expression was used as a control. Data are graphed as mean ± standard error of the mean (n = 6/group). *$p < 0.05$; **$p < 0.01$; ***$p < 0.001$; ****$p < 0.0001$

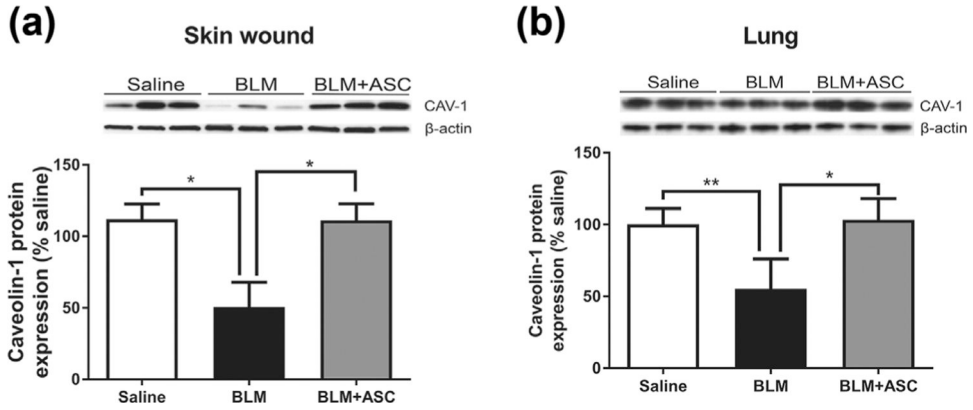

FIGURE 3.

Caveolin (CAV)-1 protein expression downregulation in lung and skin wounds of BLM-treated mice was prevented by systemic ASC treatment. Western blots were performed on skin wound (a) and lung (b) tissue from aged C57BL/6 mice treated with saline, BLM, and BLM + ASC to measure protein expression of CAV-1. BLM resulted in downregulation of CAV-1 expression compared to saline-treated controls in both skin wound and lungs. ASC treatment resulted in a prevention of this BLM-induced CAV-1 downregulation. Inset shows a representative Western blot of three mice per treatment group. Full-length blots are presented in Supplementary Figure S1. Data are graphed as mean ± standard error of the mean (n = 6/group). *$p < 0.05$; **$p < 0.01$; ***$p < 0.001$; ****$p < 0.0001$

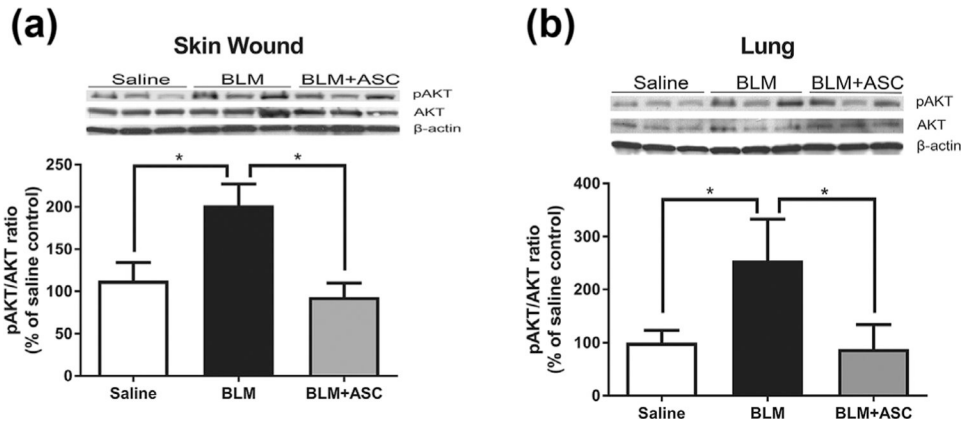

FIGURE 4.

BLM-induced activation of AKT pathway in lung and skin wounds of aged mice was prevented by ASC treatment. Ratio of phosphorylated AKT to AKT protein expression in skin wound (a) and lung (b) tissue of subjects was quantified by Western blot. Aged C57BL/6 mice treated with intratracheal BLM demonstrated increased pAKT/AKT protein expression in both tissues compared to saline-treated controls. Mice treated with intravenous infusion of allogeneic ASCs 1 day following BLM administration demonstrated decreased expression of pAKT/AKT compared to BLM-only group. Inset shows a representative Western blot of three mice per treatment group. Full-length blots are presented in Supplementary Figure S2. Data are graphed as mean ± standard error of the mean ($n = 6$/group). *$p < 0.05$; **$p < 0.01$; ***$p < 0.001$; ****$p < 0.0001$

TABLE 1

Expression of markers of fibrosis and inflammation in mice with bleomycin-induced lung injury and delayed wound healing

Group (n = 6/group)	$\alpha_v$integrin mRNA/18S	TNF-α mRNA/18S
Skin wound		
Saline	0.0806 ± 0.0193	1.641 ± 0.3802
Bleomycin only	0.4322 ± 0.1215 *	32.71 ± 13.38 *
Bleomycin + ASCs	0.0526 ± 0.0140 ****	1.352 ± 0.2375 ***
Lung		
Saline	0.5343 ± 0.1569	8.714 ± 1.786
Bleomycin only	1.484 ± 0.2556 **	15.22 ± 2.168 *
Bleomycin + ASCs	0.4048 ± 0.2964 ***	5.701 ± 2.649 ***

ASCs, adipose-derived mesenchymal stem cells.

* $p < 0.05$ versus saline;

** $p < 0.01$ versus saline;

*** $p < 0.05$ versus BLM only;

**** $p < 0.01$ versus BLM only.